

1 Peanut oral immunotherapy differentially suppresses clonally distinct 2 subsets of T helper cells

3 Author List: Brinda Monian^{1,2,*}, Ang A. Tu^{1,3,*}, Bert Ruiter^{4,5}, Duncan M. Morgan^{1,3}, Patrick M.
4 Petrossian¹, Neal P. Smith^{4,5}, Todd M. Gierahn¹, Julia H. Ginder¹, Wayne G. Shreffler^{4,5,**}, J.
5 Christopher Love^{1,2,6,**}

6 Author Affiliations:

7 ¹Koch Institute for Integrative Cancer Research, Massachusetts Institute of Technology,
8 Cambridge, MA, USA

9 ²Department of Chemical Engineering, MIT, Cambridge, MA, USA

10 ³Department of Biological Engineering, MIT, Cambridge, MA, USA

11 ⁴Center for Immunology and Inflammatory Diseases, Massachusetts General Hospital, Boston,
12 MA, USA

13 ⁵Harvard Medical School, Boston, MA, USA

14 ⁶Broad Institute of MIT and Harvard, Cambridge, MA, USA

15 *These authors contributed equally.

16 **These authors contributed equally.

17

18 **Abstract**

19 Food allergy affects an estimated 8% of children in the US, with increasing severity and global
20 prevalence¹. Oral immunotherapy (OIT) is a recently approved treatment with outcomes ranging
21 from sustained tolerance to food allergen to no apparent benefit^{2,3}. The immunological
22 underpinnings that influence clinical outcomes of OIT still remain largely unresolved. Using single-
23 cell RNA sequencing and paired TCR α/β sequencing, we assessed the transcriptomes of
24 CD154+ and CD137+ peanut-reactive T helper cells from 12 peanut-allergic patients
25 longitudinally throughout OIT. We observed expanded populations of cells expressing Th1, Th2,

26 and Th17 signatures that further separated into six clonally distinct subsets, including a Tfh1-like,
27 a Tfh2-like, a Th2A-like, and a Th2reg-like subset. Four of these subsets demonstrated
28 convergence of TCR sequences, suggesting antigen-driven T cell fate. Although we observed
29 suppression during OIT of Th2 and Th1 gene signatures within effector clonotypes, Tfh clonotypes
30 were unaffected. We also did not observe significant clonal deletion or induction among the
31 antigen-reactive T cells characterized. Positive outcomes were associated with larger decrease
32 of Th2 signatures in Th2A-like cells, while treatment failure was associated with high baseline
33 inflammatory gene signatures that were unmodulated by OIT. These signatures, including
34 expression of *OX40*, *OX40L*, *STAT1*, and *GPR15*, were most clearly present in Th1 and Th17
35 clonotypes, but were also more broadly detected across the CD154+ CD4 population. These
36 results demonstrate that differential clinical response is associated both with pre-existing trait
37 characteristics of the CD4 immune compartment and with susceptibility to modulation by OIT.

38

39 **Conflict of Interest Statement**

40 A.A.T., T.M.G., J.C.L., and the Massachusetts Institute of Technology have filed patents related
41 to the single-cell sequencing methods used in this work. J.C.L. has interests in Sunflower
42 Therapeutics PBC, Pfizer, Honeycomb Biotechnologies, OneCyte Biotechnologies, SQZ
43 Biotechnologies, Alloy Therapeutics, QuantumCyte, Amgen, and Repligen. J.C.L.'s interests are
44 reviewed and managed under Massachusetts Institute of Technology's policies for potential
45 conflicts of interest. J.C.L. receives sponsored research support at MIT from Amgen, the Bill &
46 Melinda Gates Foundation, Biogen, Pfizer, Roche, Takeda, and Sanofi. The spouse of J.C.L. is
47 an employee of Sunflower Therapeutics PBC. T.M.G. is currently an employee of Honeycomb
48 Biotechnologies, Inc. A.A.T. is currently an employee of Immunitas Therapeutics, Inc. W.G.S. is
49 a consultant of Aimmune Therapeutics.

50

51 Introduction

52 Food allergy is an immune hypersensitivity condition characterized by high-affinity allergen-
53 specific IgE antibodies and allergen-specific Th2 cells^{2,4}. Specific IgE binds to effector cells, such
54 as mast cells and basophils, through FcεRI receptors that are cross-linked upon binding of
55 allergen. The resulting cellular degranulation causes local and systemic release of histamine and
56 other mediators, leading to allergic reactions ranging from mild symptoms, such as hives and
57 abdominal pain, to potentially life-threatening anaphylaxis⁵. Allergen-specific Th2 cells constitute
58 a critical component in this cascade of events. Th2 cells are broadly defined by the expression of
59 the transcription factor GATA3 and the secretion of cytokines IL-4, IL-5, and IL-13, which promote
60 class-switching of B cells to IgE and recruitment of eosinophils as well as other effector cells^{6,7}.
61 Recent studies have highlighted subtypes of Th2 cells with specialized functions in the context of
62 allergy, including effector memory (e.g. Th2A, peTh2), and T follicular helper (e.g. Tfh13)
63 phenotypes⁷⁻¹².

64
65 Oral immunotherapy (OIT) is currently the only FDA-approved treatment for food allergy intended
66 to prevent anaphylaxis³. OIT involves the daily ingestion of escalating doses of allergen. Most
67 patients (80-85%) achieve desensitization (a loss in clinical reactivity with regular consumption of
68 allergen), but only about a third of patients maintain unresponsiveness if treatment is discontinued
69 for even just a few months¹³⁻¹⁵. Studies of the impact of OIT on circulating T cells have consistently
70 found evidence for suppression of Th2 responses, but most of these studies have not correlated
71 T cell responses with heterogenous clinical outcomes^{8,16-19}. Similarly, while regulatory T cell
72 (Treg) induction has been observed using *in vitro* expansion of T cells from OIT patients, it has
73 not been consistently shown *ex vivo*¹⁸⁻²⁵. Studying allergen-reactive T cell subsets *ex vivo* is
74 challenging due to their low frequencies in peripheral blood and technical limitations to both
75 reliably phenotype these populations and track corresponding clonotypes longitudinally^{23,26}. As a
76 result, existing data on T cell responses in the context of OIT have been limited to features

77 comprising a narrow set of genes and proteins or cells specific to a pre-defined subset of allergen
78 epitopes. Comprehensive characterization of allergen-specific CD4+ T cell subsets and their
79 response to immunotherapy over time may not only refine treatment strategies for food allergy,
80 but also enhance our broader understanding of T helper cell phenotypes in atopic disease.
81

82 **Results**

83 **Single-cell RNA-Seq enables deep profiling of peanut-reactive T helper cells from OIT**
84 **patients.** To measure the impact of OIT on peanut-reactive T cells, we profiled longitudinal blood
85 samples from 12 patients participating in a clinical trial of peanut OIT (NCT01750879,
86 **Supplementary Table 1,2**). In brief, PBMCs were isolated at four timepoints from each patient:
87 baseline (BL; before therapy), buildup (BU; 13 weeks after start of therapy), maintenance (MN;
88 12 weeks after the maximum dose was reached), and avoidance (AV; 12 weeks after the end of
89 therapy). Clinical outcomes were evaluated by two oral food challenges and were defined as:
90 tolerance (TO) - passing both food challenges; partial tolerance (PT) - passing the maintenance
91 challenge but failing the avoidance challenge; and treatment failure (TF) - failing the maintenance
92 challenge. Samples from three placebo group (PL) patients were also included (**Figure 1A**;
93 **Methods**).

94
95 To enrich for allergen-specific T cells and capture their activated profiles, we cultured the PBMCs
96 with whole peanut protein extract for 20 hours to activate CD4⁺ memory T cells. Peanut-reactive
97 cells were then enriched via FACS using CD154 and CD137 (activation markers for T_H17 and T_H1
98 states, respectively) (**Figure 1A**; **Supplementary Figure 1A**). This approach allowed us to
99 recover a broad set of peanut-specific T cells with limited bias for specific epitopes or HLA types²⁷.
100 The relatively short stimulation time was intended to capture *ex vivo* cell states and reflect *in vivo*
101 clonal distributions²⁸. CD154-based approaches have been broadly used to identify antigen-
102 reactive CD4⁺ T cells in various contexts^{26,29,30}. In addition, we have previously shown that the
103 frequency of peanut-reactive CD4⁺ T cells, identified by CD154 expression, is correlated with
104 severity of peanut allergy¹¹. Using this method, we observed that OIT significantly decreased the
105 frequency of peanut-reactive CD154⁺ and CD137⁺ T cells in the peripheral blood.
106 (**Supplementary Figure 1B**). To further characterize the peanut-reactive memory CD4⁺ T cells
107 and study how their phenotypes and repertoire are altered during OIT in relation to treatment

108 outcome, we processed the sorted cells for single-cell RNA-Seq via Seq-Well and paired single-
109 cell TCR α/β sequencing^{31,32}. In total, we recovered high-quality transcriptomes for 134,129 cells
110 (74,646 CD154+, 41,186 CD137+, and 18,297 CD154-CD137-; **Methods; Supplementary**
111 **Figure 2**).

112

113 Peanut-reactive T cell transcriptomes formed clusters associated most closely with their sorted
114 subsets (**Figure 1B**). CD154+ and CD137+ cells were separated as expected by several
115 differentially expressed genes, including their associated transcripts *CD40LG* and *TNFRSF9*, and
116 other transcripts consistent with their respective effector or regulatory phenotypes (**Extended**
117 **Data Figure 1A**). We observed patient-specific variation within each cluster that was not a
118 function of library size or mitochondrial content (**Figure 1B; Supplementary Figure 2B**),
119 suggesting that it represented inherent biological rather than technical differences. Qualitatively,
120 there was no strong association between transcriptome (as measured by UMAP embedding) and
121 time point or treatment outcome, suggesting that OIT-induced effects might be subtle rather than
122 dominant in the data.

123

124 **Sparse PCA delineates canonical and new T-helper cell gene modules.** To uncover evidence
125 of OIT-driven variation among peanut-reactive T cells, we developed an unsupervised approach
126 to identify conserved programs of immune-related gene expression. The dataset was filtered to
127 937 immune and variable genes (**Supplementary Table 3**). Then, co-expressed genes were
128 aggregated into gene modules using sparse principal components analysis (PCA)³³ to derive a
129 set of 50 gene modules (**Methods; Supplementary Figure 3,4**). Several modules corresponded
130 well with the phenotypes of known T cell subsets, such as Th1, Th2, Th17, and regulatory T cells
131 (**Figure 1C**). 43 out of 50 gene modules were present across most or all patients (**Supplementary**
132 **Figure 5; Methods**), suggesting that these represent programs of T cell function or activation that
133 are consistent among individuals.

134

135 **Th-related gene modules are associated with expanded T cells.** To investigate clonal T cell
136 responses to peanut antigens, we recovered paired TCR sequences from the single-cell
137 transcriptomic sequencing libraries. We identified TCR β sequences for 60% (+/-17%), TCR α for
138 55% (+/-15%) and both chains for 36% of cells (+/- 12%) (numbers represent median +/- standard
139 deviation across patients). Coverage was uniform across samples, and the majority of expanded
140 TCR β sequences were paired with a single TCR α (**Figure 2A**; **Supplementary Figure 6**). Given
141 this relationship, we used TCR β for all subsequent analyses involving clonotypes. The diversities
142 of CD154+ and CD137+ repertoires were significantly lower than those of the CD154-CD137-
143 cells, indicating that these activation markers enriched for a pool of clonally expanded, peanut-
144 reactive clonotypes (**Figure 2B, C**). In addition, we observed that 55% of expanded clones were
145 detected across multiple time points, but only 1.6% of clonotypes were shared between CD154+
146 and CD137+ cells, suggesting that these two activated subsets resulted from fundamental
147 differences in lineage, epitope specificity, or both (**Figure 2D**).

148

149 To determine which, if any, gene modules were associated with clonal T cell expansion, we
150 classified cells as expressing or non-expressing for each module, based on whether the module
151 score was above background expression in CD154-CD137- cells (**Methods**). We then calculated
152 the average TCR β clonal size for cells expressing each module, as well as the average score of
153 that module in CD154+ cells relative to CD154-CD137- cells. We found that modules representing
154 Th1, Th2, and Th17 functions exhibited strong upregulation in both the CD154+ and CD137+
155 compartments and were associated with expanded T cell clonotypes (**Figure 2E**; **Extended Data**
156 **Figure 1**).

157

158 **T helper cells comprise six clonally distinct subtypes.** Due to their strong enrichment in the
159 CD154+ and CD137+ compartments, we further analyzed the heterogeneity among cells
160 expressing the Th1, Th2, and Th17 modules. Separate clustering of these cells revealed three
161 phenotypically distinct clusters of Th2 cells and two clusters of Th1 cells. We did not observe
162 additional clusters within the Th17 cells (**Figure 3A**). These clusters were detected in all patients
163 (**Supplementary Figure 7C**). Within the Th2 cells, the clusters corresponded to a Tfh2-like (high
164 in costimulatory markers, *CXCR5*, and *PDCD1*), a Th2reg-like (*FOXP3* and *TNFRSF9*), and a
165 Th2A-like population^{8,34} (*GATA3*, *IL17RB*, and *PTGDR2*; **Figure 3B**). The Tfh2-like population
166 resembled a previously-described pathogenic Tfh13 subset, while the Th2A-like population
167 shared markers previously identified in Th2A and peTh2 populations⁸⁻¹⁰ (**Supplementary Figure**
168 **8**). Likewise, the Th2reg-like population shared features with previously described deviated Treg
169 cells in food allergy³⁵. Among the Th1 cells, the clusters corresponded to a Tfh1-like population
170 and a Th1-conv (conventional) population with canonical Th1 signatures³⁶ (**Figure 3A, B**). Both
171 of these clusters expressed high levels of *IFNG* and *GZMB*, and the Tfh1-like cluster exhibited
172 high overlap of genes also expressed in the Tfh2-like population, including *ICOS*, *PDCD1* and
173 *TNFRSF9*.

174
175 Analysis of the TCR repertoires of the six T-helper subtypes showed that most clones were
176 primarily associated with a single subtype, indicating that these populations represent distinct
177 clonal lineages (**Figure 3C**). We did, however, observe overlapping clones between the Th1-conv
178 and Th17 states as well as the Tfh1-like and Tfh2-like states, suggesting that cells may transition
179 between these pairs of phenotypic states, or that these states may include shared cellular
180 lineages that differentiated relatively late³⁷.

181
182 To determine to what extent this association between clonotype and phenotype might be
183 influenced by epitope recognition, we next assessed whether or not TCRs showed evidence of

184 convergence within T helper subtypes using TCRdist, a quantitative metric for similarity between
185 a pair of TCR sequences³⁸ (**Methods**). A pair of cells with very similar TCR sequences may share
186 epitope binding properties despite having different ancestries, allowing an assessment of the role
187 of epitope recognition in shaping T cell phenotypes. We found that pairs of cells with highly similar
188 TCR β sequences (TCRdist < 9) had a significantly enriched likelihood of both cells belonging to
189 the same T helper subtype ($p < 0.05$ by a Chi-square proportion test), with the exception of cells in
190 the Th2A-like and Th2reg-like subtypes (**Figure 3D**). This result indicates a convergence onto
191 common TCR motifs within most subtypes and suggests that factors such as TCR affinity or
192 antigen context during priming (e.g. local tissue environment) may influence the induction of
193 specific T helper phenotypes within an individual^{39–41}.

194

195 **OIT suppresses Th2 and Th1 signatures in conventional effector, but not Tfh-like, cells.**

196 We next assessed the impact of OIT on the TCR repertoire and the identified T helper subtypes.
197 The majority of expanded CD154+ and CD137+ clonotypes were present at three or four of the
198 timepoints, and no timepoint was associated with the depletion or emergence of unique expanded
199 clonotypes or singletons, suggesting that OIT does not induce strong changes in peanut-reactive
200 TCR repertoires (**Extended Data Figure 2**). To investigate the impact of OIT on functional T cell
201 phenotypes, we assessed the mean expression of Th1, Th2, and Th17 modules in all CD154+
202 cells from each patient and found evidence of suppression at the bulk-level in Th2 and, to a lesser
203 extent, Th1 module scores (adjusted p-values of 0.036 and 0.117, respectively) between the
204 baseline and maintenance timepoints (**Figure 4A**). This was not observed in patients treated with
205 placebo (**Supplementary Figure 9B**).

206

207 We then quantified the impact of OIT on gene module expression by individual clonotype in each
208 of the T helper subtypes. This analysis allowed us to track the phenotypes of hundreds of
209 individual clonal lineages over the course of treatment. To understand the stability of module

210 expression over time within a clonotype, we calculated the “fractional clonal expression” for each
211 clonotype by assigning it to the T helper subset in which it most frequently appeared, and then
212 tabulating the proportion of cells that expressed the corresponding module (Th2, Th1, or Th17) at
213 each time point (**Methods**). We found that Th1-conv and Th2A-like clonotypes had suppressed
214 expression of Th1 and Th2 genes, respectively, at the maintenance time point compared to
215 baseline. This suppression was consistent with an anergic state, characterized by decreased
216 cytokine expression in response to stimulation, and was not detected in the placebo group
217 (**Supplementary Figure 9C**). In contrast, we did not observe statistically significant changes in
218 module expression at the clonotype-level in the Tfh1-like, Tfh2-like, Th2reg-like, or Th17 subsets
219 (**Figure 4B; Supplementary Figure 9C**), suggesting that these populations are more refractory
220 to modulation by OIT than Th1-conv and Th2A-like clonotypes. A lack of suppression of Th2A-
221 like clonotypes at maintenance was associated with treatment failure (Spearman’s rho of 0.74
222 and unadjusted p-value of 0.02), although the degree of suppression did not differ between partial
223 and full tolerance groups (**Figure 4C**). No statistically significant association was found in Th1-
224 conv clonotypes (**Supplementary Figure 9A**).

225
226 **Non-Th2 inflammatory pathways at baseline are associated with clinical outcome.** While a
227 lack of Th2 suppression during OIT was associated with poor clinical outcome, its baseline
228 expression was not predictive. To analyze immune signatures prior to the start of treatment, we
229 performed PCA on gene module scores of all CD154+ cells at baseline. This approach allowed
230 us to assess major axes of phenotypic variation among CD154+ cells at baseline and investigate
231 whether any of these axes correlate with clinical outcome. We found a striking separation by
232 outcome at all timepoints in the scores of the first principal component (PC1) alone, with high PC1
233 scores associated with poor clinical outcome (**Figure 4D**). The top gene modules enriched in PC1
234 were defined by markers of T cell activation and effector response such as OX40, OX40L, Th17
235 function, STAT1, and GPR15 (**Figure 4E; Supplementary Figure 10**). To investigate the cell

236 types associated with this signature, we summarized PC1 scores and module expression in the
237 six previously identified Th subtypes. Of these, Th1-conv and Th17 cells expressed the highest
238 levels of PC1 (**Supplementary Figure 11**). Consistent with this observation, the frequencies of
239 Th1-conv and Th17, but not Th2, cells were also lower in patients with favorable clinical outcome
240 within the CD154+ compartment (**Supplementary Figure 7**). Interestingly, CD154+ cells not
241 classified within any of the canonical CD4 T cell subtypes also showed outcome-dependent
242 expression of modules associated with PC1 (**Supplementary Figure 10; Supplementary Figure**
243 **12**). These results indicate that a range of CD4 T cell phenotypes and inflammatory pathways
244 may impact the likelihood of favorable responses to OIT.

245

246 **Discussion**

247 In this study, we characterized peanut-reactive T helper cells from allergic patients undergoing
248 OIT using single-cell RNA sequencing with paired TCR sequencing. These methods allowed us
249 to identify patterns of expansion and TCR convergence among distinct peanut-reactive T helper
250 subtypes and to longitudinally profile individual clonotypes throughout OIT. We found differential
251 effects of OIT on T helper subtypes and a significant association at baseline between T cell
252 phenotypes and clinical outcome, that is unmodulated by OIT. Our results add refinement to the
253 transcriptomic-scale definitions of previously described subsets, reveal how clonotypes from
254 these populations are affected during OIT, and provide additional insight into the substantial
255 heterogeneity of peanut allergic patients.

256

257 Among sorted CD154+ and CD137+ T helper cells, we identified six subtypes of highly clonal
258 peanut-reactive T helper cells with Th1, Th2, and Th17 signatures. Of these subtypes, the Th2A-
259 like, Tfh2-like, and Th2reg-like cells correspond well to the previously described Th2A, Tfh13, and
260 deviated Treg populations in food allergy^{8-10,35}. We show here for the first time that these subsets
261 have distinct TCR repertoires and that some are enriched in highly similar TCR sequences. Our

262 results add resolution to a previous study showing that distinct repertoires exist between CD154+
263 and CD137+ cells²⁷. This segregation of TCR repertoires strongly suggests that the subsets
264 represent distinct lineages rather than transient phenotypes, and the phenomenon of TCR
265 convergence hints at the skewing of T cell state due to epitope interactions or epitope-associated
266 factors⁴¹⁻⁴³. We did not detect significant TCR convergence in the Th2A-like and the Th2reg-like
267 subsets, which could be due to the higher diversities of repertoires in these subsets that would
268 require deeper sampling to detect any convergence.

269

270 We also showed, for the first time, how these three Th2 subsets, as well as Th1 and Th17 cells,
271 responded over the course of OIT. Globally, we found that OIT induced a transient reduction of
272 the frequency of CD154+ T cells and the mean expression of Th2 signatures in response to
273 peanut antigen stimulation. However, we also found that the TCR repertoires of peanut-reactive
274 Th2 cells were stable over time, suggesting that OIT acts predominantly via suppression of
275 functional phenotypes rather than by clonal deletion or TCR-biased sequestration away from the
276 periphery. This result corroborates two previous studies that reported the emergence of anergic
277 signatures in peanut-specific T cells over time in OIT, and provides insight into previous reports
278 of decreases in circulating Th2 frequency following OIT^{8,18,19,22,23}. Furthermore, we observed OIT-
279 induced suppression among Th2A-like and Th1-conv, but not Tfh-like, clonotypes. Finally, we
280 observed that the suppression of Th2 module expression in Th2A-like clonotypes was associated
281 with clinical outcome. Our findings indicate that OIT is successful in modulating only a subset of
282 peanut-reactive T cells, and that the T cells most responsible for Ig class-switching and B cell help
283 may be the least altered by treatment, highlighting the difficulty of achieving a sustained change
284 in clinical outcome.

285

286 With respect to therapeutic outcomes, we found that an unsupervised composite score of all gene
287 modules, derived using only data from cells isolated before treatment (baseline), corresponded

288 strongly with treatment failure and was not modulated by treatment. This score was driven largely
289 by markers of T cell activation such as *OX40*, *OX40L*, and *STAT1*, as well as Th1 and Th17 genes
290 (**Supplementary Figure 10C**). We surmise that high levels of baseline T cell activation could limit
291 the effectiveness of OIT due to increased inflammation or altered gastrointestinal permeability
292 (potentially triggered by Th17 responses⁴⁴). Assessments of genomic or immunologic features
293 associated with clinical outcomes in OIT are scarce, but Th17 cells have been reported to play a
294 role in atopic disease, with some preliminary evidence suggesting that they are modulated by
295 OIT^{26,45–47}. Similarly, OX40 and OX40L have also been implicated in atopic dermatitis and asthma,
296 and represent a possible therapeutic target^{48,49}.

297
298 Moreover, while some of the top gene modules in the composite score were highly enriched
299 among Th1 and Th17 subsets (e.g., the OX40L module), many were also expressed in other
300 compartments of CD154+ or CD137+ cells (**Supplementary Figure 10**), including CD154+ cells
301 not classified as any of the Th subtypes. Such was the case for the GPR15 and STAT1 signaling
302 modules (**Supplementary Figure 12**). GPR15 has been highlighted as a colon-homing receptor
303 in CD4+ T cells, and STAT1 (along with GBP4 and GBP1, also included in the same module) is
304 associated with response to interferon^{50,51}. Taken together, these results could suggest that
305 altered gastrointestinal permeability and inflammatory responses in diverse combinations of
306 peanut-reactive T cells may influence the likelihood of responding favorably to OIT.

307
308 Tregs have been described in some studies as a correlate of favorable clinical outcome in OIT^{20,21}.
309 While we detected a strong and sustained expression of Treg markers among peanut-reactive
310 CD137+ cells, we actually saw a moderate decrease in the frequency of CD137+ cells over the
311 course of OIT (**Supplementary Figure 1B**). In addition, although *IL10* in both CD137+ and
312 CD154+ was transiently induced, there was neither a sustained increase in Treg expression
313 among CD137+ cells over OIT, as measured by the average level of expression of the Treg

314 module or *FOXP3* and *IL10* (**Extended Data Figure 3**), nor a correlation of *IL10* or *FOXP3* with
315 clinical outcome. Finally, we did not see evidence for the induction of new peanut-reactive Treg
316 clonotypes during OIT, as TCR repertoires of CD137+ cells remained stable over time (**Extended**
317 **Data Figure 2**). Discrepancies between our results and those of prior studies could reflect
318 differences in stimulation conditions and strategies for identifying antigen-specific Tregs, and they
319 motivate further efforts towards elucidating the role of peanut-reactive Tregs in OIT.

320

321 The methods we used in this study combine FACS-based enrichment of activated T cells with
322 single-cell RNA-Seq and TCR sequencing as a framework for profiling antigen-reactive T cells
323 without the use of tetramer reagents. By enriching peanut-reactive T cells based on CD154 and
324 CD137 expression, it is likely that our data include some fraction of non-specific activated T cells.
325 By integrating data on TCR sequences, however, we identified T cell states that were associated
326 with both clonal expansion and peanut-antigen activation, thereby minimizing the effects of non-
327 specifically activated T cells. We believe this framework could be used to identify likely antigen-
328 reactive T cells in other disease contexts.

329

330 We believe this work has implications for the study of human T cell biology as well as mechanisms
331 of OIT. First, the methodology implemented here provides a framework for the design and
332 analysis of paired TCR and transcriptome data of antigen-reactive T cells, and this substantial
333 dataset of human single-cell data provides a useful reference for future studies. Using this
334 framework, we detected significant heterogeneity within the peanut-reactive CD154+ T cell
335 compartment and highlighted potential roles for TCR-epitope interactions in skewing T cell
336 phenotype. Second, our data have revealed several features of OIT that merit further
337 investigation. Based on our data, OIT does not appear to delete peanut-reactive Th2 clones; these
338 findings point to selective clonal suppression, rather than deletion, as a major mechanism of OIT
339 and highlight why sustained tolerance may be difficult to achieve. Furthermore, we found that

340 failure to respond to OIT was reflected in a broad baseline activation signature, highly expressed
341 in Th17 and other T cells, that was resistant to modulation by OIT. In the future, prospective OIT
342 studies could evaluate this signature as a predictor of treatment success. In summary, we used
343 single-cell RNA-Seq and TCR clonotyping to reveal a complex set of highly distinct T helper cell
344 phenotypes, beyond effector Th2, that are relevant to the efficacy of OIT. Future therapeutic
345 modalities that either target these diverse phenotypes and inflammatory pathways, such as Tfh,
346 Th17, OX40-OX40L, or that appreciably delete peanut-specific Th2A cells, may be more likely to
347 promote sustained tolerance in food allergy than allergen-based approaches alone.

348

349 **Author Contributions**

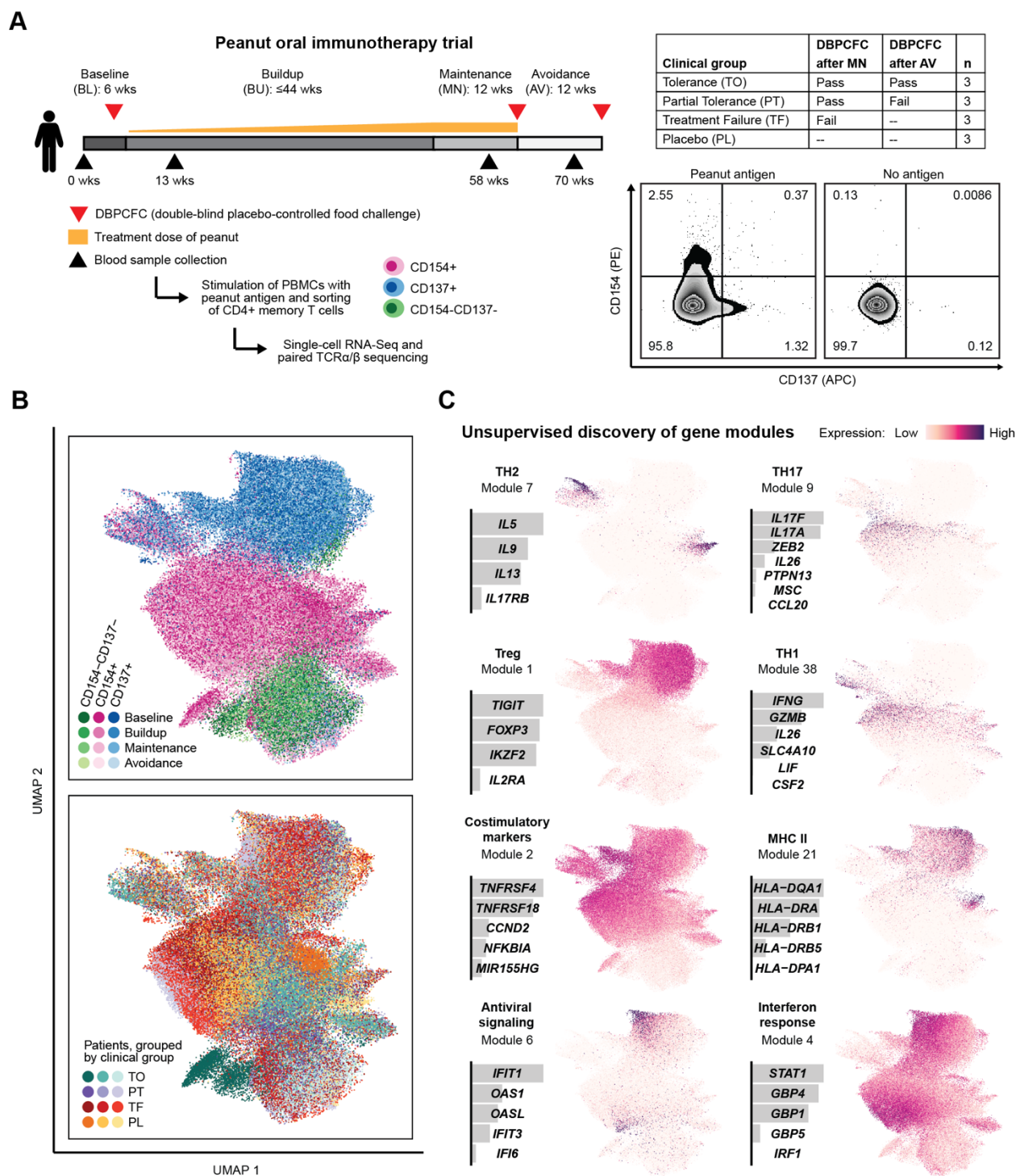
350 W.G.S. and J.C.L. conceptualized the study. W.G.S. conducted the clinical trial (NCT01750879).
351 B.M., A.A.T., B.R., and P.M.P. conducted experiments. B.M., A.A.T., D.M.M., and N.P.S.
352 analyzed the data. T.M.G. and J.H.G. conducted experiments to develop and validate methods.
353 B.M., A.A.T., B.R., D.M.M., W.G.S., and J.C.L. wrote and edited the manuscript.

354

355 **Acknowledgements**

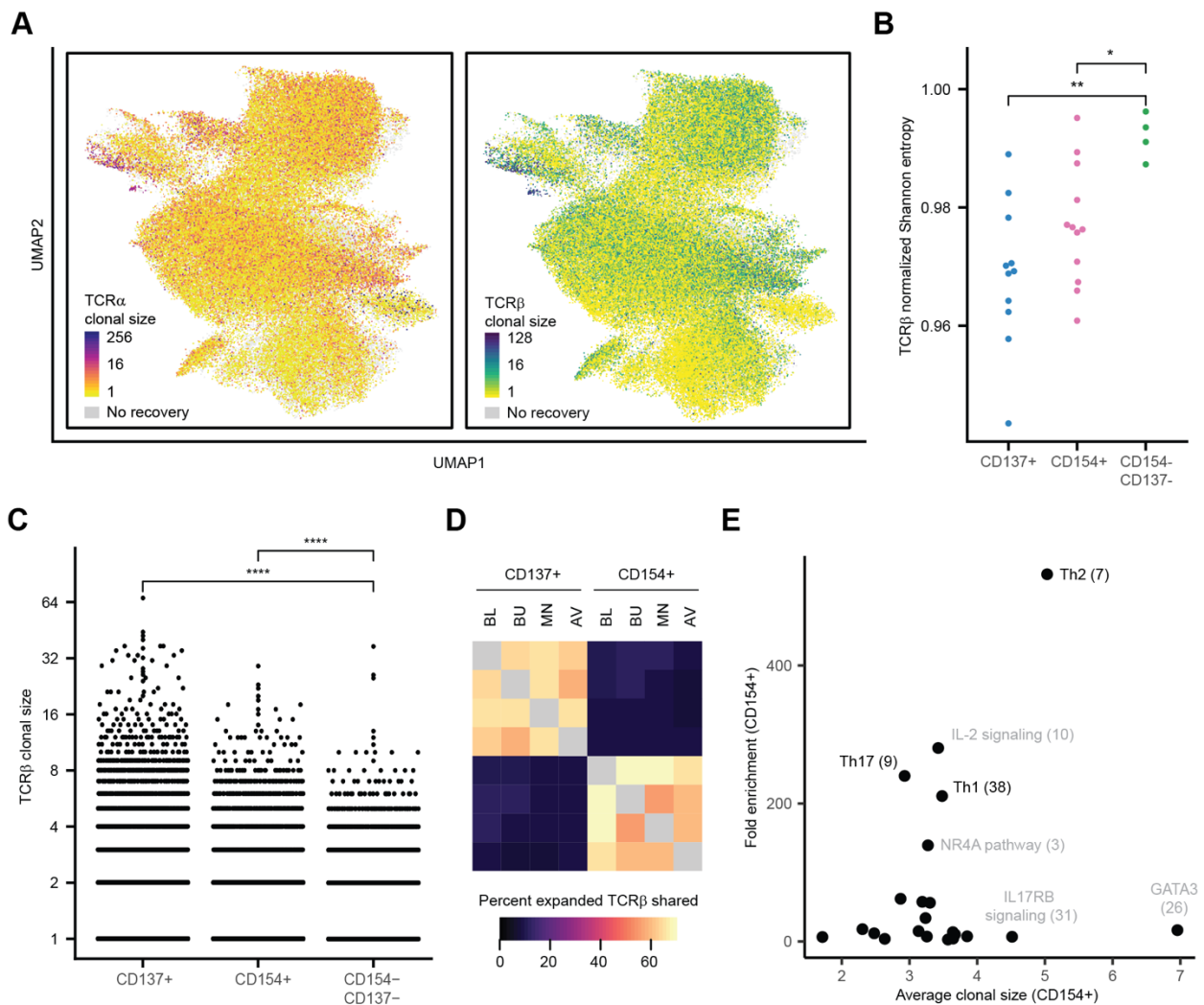
356 We would like to thank our patients and their families who generously gave their time and
357 participation, as well as Lauren Tracy, Colby Rondeau, Christine Elliot and Leah Hayden, the
358 clinical coordinators of this study. We would also like to thank Sarita U. Patil and Yamini V. Virkud
359 for fruitful discussions. The clinical work was performed in the Harvard Clinical and Translational
360 Science Center supported by grants 1UL1TR001102 and 8UL1TR000170 from the National
361 Center for Advancing Translational Sciences, and 1UL1RR025758 from the National Center for
362 Research Resources. In addition, we thank our colleagues at the MGH Department of Pathology
363 Flow and Image Cytometry Research Core for their help with cell sorting. The Flow Core obtained
364 funding from the National Institutes of Health Shared Instrumentation program (1S10OD012027-
365 01A1, 1S10OD016372-01, 1S10RR020936-01, and 1S10RR023440-01A1). This work was

366 supported in part by the Koch Institute Support (core) NIH Grant P30-CA14051 from the National
367 Cancer Institute, as well as the Koch Institute - Dana-Farber/Harvard Cancer Center Bridge
368 Project. This work was also supported by the Food Allergy Science Initiative at the Broad Institute
369 and the NIH (5P01AI039671, 5U19AI089992, U19AI095261).



371
 372 **Figure 1. Peanut-reactive T cells from individuals undergoing OIT have diverse**
 373 **transcriptional signatures.** a, OIT study design, definition of clinical outcomes, and
 374 representative flow plots from one patient at baseline. CD3+CD4+CD45RA- memory T cells were
 375 sorted by FACS as CD154+CD137+/- ("CD154+"), CD154-CD137+ ("CD137+"), or CD154-
 376 CD137-.

377 sorted subset and time point (top) or by patient and clinical group (bottom). **c**, Selected gene
378 modules discovered using sparse principal components analysis. For each module, a description,
379 the relative weights of each contributing gene, and the module score of all cells overlaid on the
380 UMAP coordinates are shown.



382

383 **Figure 2. Gene modules for T helper function are associated with clonal expansion and**

384 **expression in activated cells. a**, Clonal size of TCR α sequence (left) or TCR β sequence (right)

385 for all cells with paired TCR recovery, overlaid onto UMAP coordinates. Clonal size is defined as

386 the number of cells sharing a TCR sequence. **b**, Normalized diversity (Shannon index) of TCR β

387 repertoires of each sorted subset. Each data point represents the repertoire of one patient at all

388 time points. ‘***’ refers to an adjusted p-value of <0.01 by Wilcoxon rank-sum test, and ‘*’ refers to

389 an adjusted p-value of <0.05. **c**, Distribution of TCR β clonal sizes, within each sorted subset.

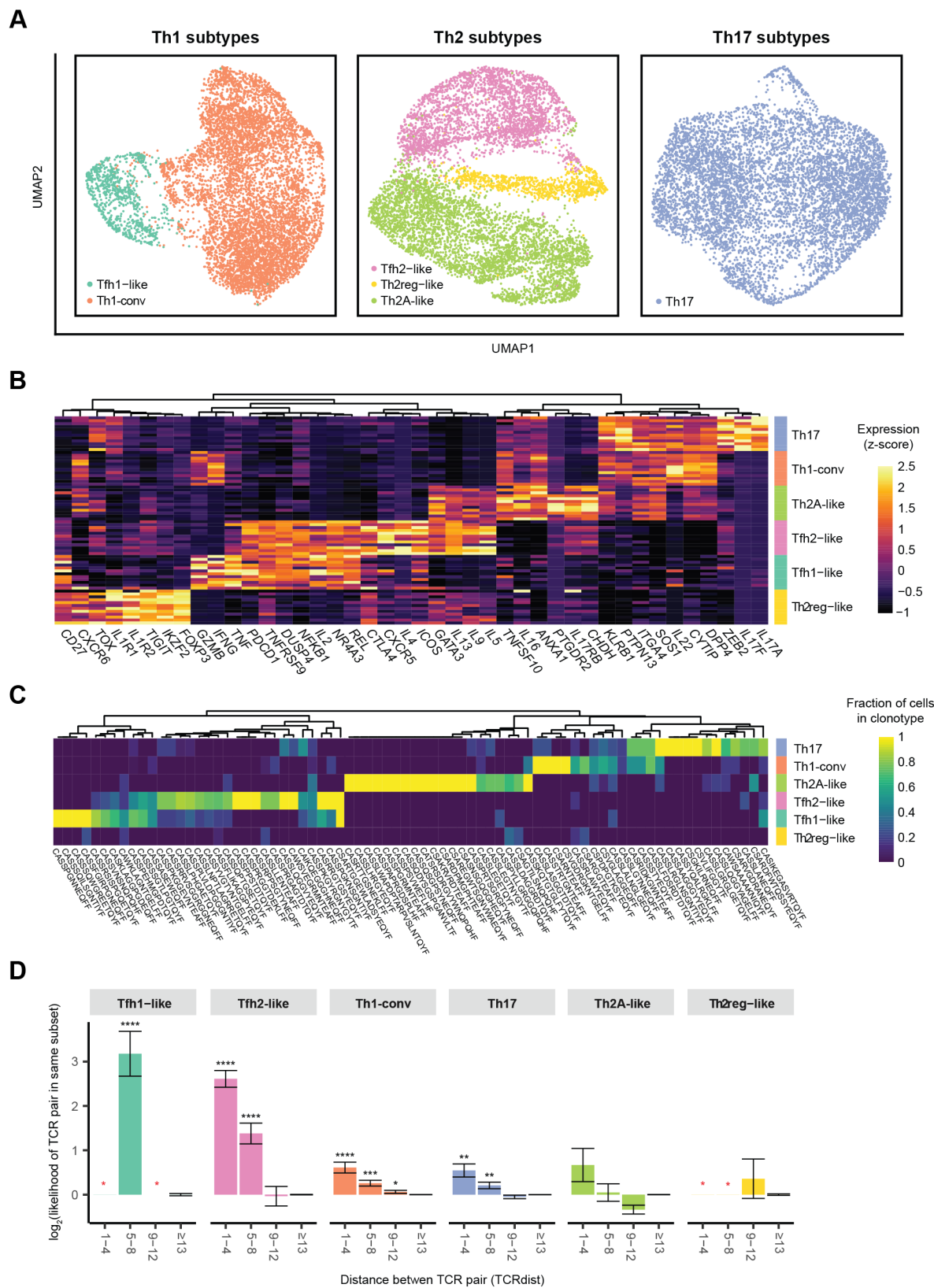
390 ‘****’ refers to an adjusted p-value of <0.0001 by Wilcoxon rank-sum test. **d**, Percent of TCR β

391 sequences shared between time points and sorted subsets. ‘Percent shared’ is defined as the

392 number of unique TCR β sequences detected in both conditions, divided by the geometric mean

393 of the number of unique TCR β sequences in each of the two conditions. Sequences from all

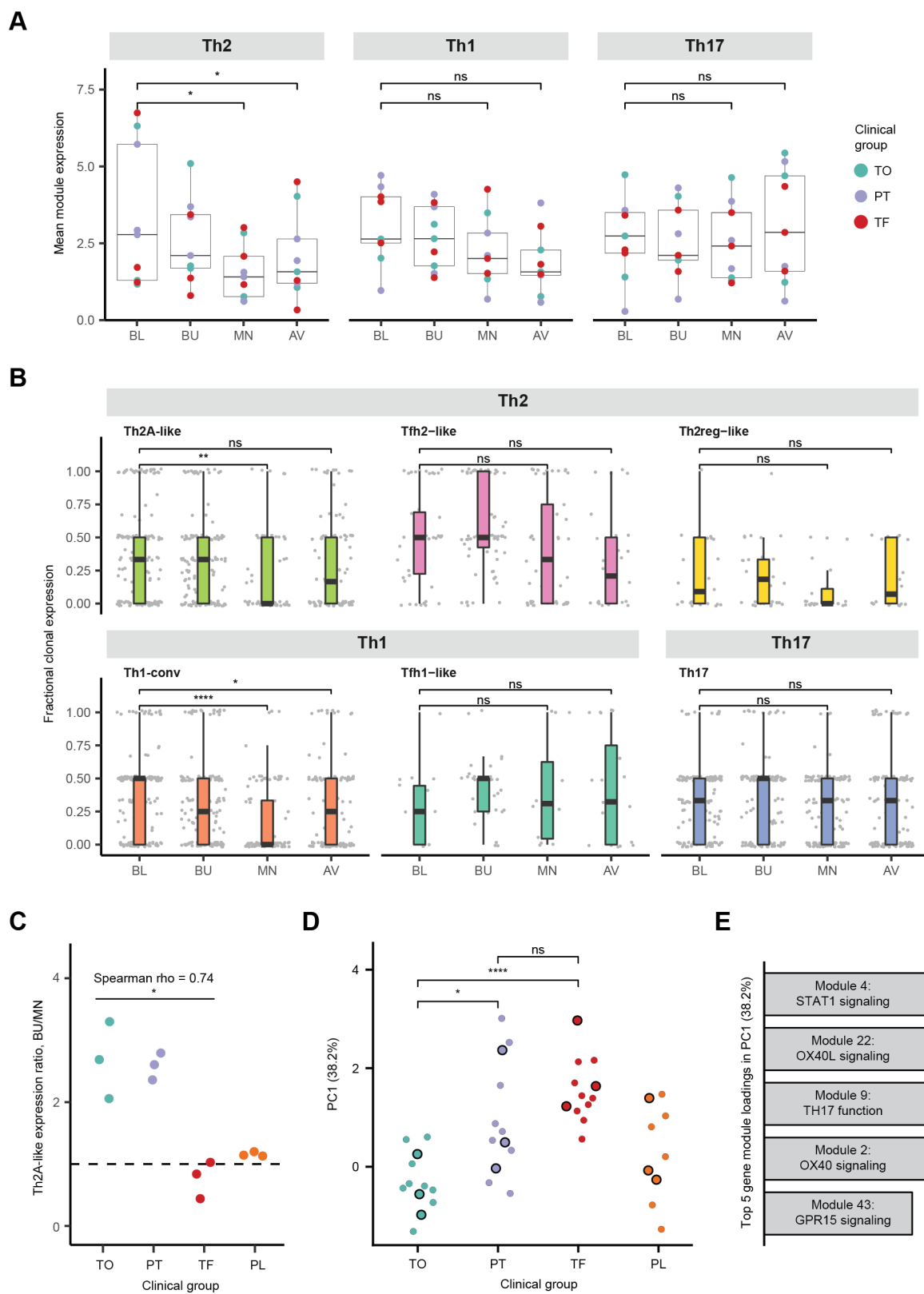
394 treatment-group patients were pooled. **e**, Mean clonal size and fold-change in mean module
395 scores (compared to module-expressing CD154-CD137- cells) in CD154+ cells expressing each
396 gene module. Cells were classified as ‘expressing’ each module or not, relative to background
397 expression (**Methods**). Clonal size was calculated with respect to all cells in the dataset.



399

400 **Figure 3. Peanut-reactive T helper subtypes are clonally distinct and exhibit TCR**
 401 **convergence.** **a**, UMAP visualizations of Th1-, Th2-, and Th17-scoring cells. Clusters are
 402 annotated by their putative identity. **b**, Differentially expressed genes in each T helper subset.

403 Genes were selected using ROC test and manual curation. Each row represents the scaled
404 average gene expression in one patient. **c**, Fraction of TCR β clonotypes belonging to each
405 subset. Fraction is defined as the number of cells of a TCR β sequence (column) detected in each
406 subset, divided by the total number of cells within the clonotype. Clonotypes were randomly
407 downsampled to visualize a comparable number from each subset. **d**, TCR distance analysis of
408 TCR β sequences in the subsets. x-axis represents bins of increasing pairwise TCR distance,
409 calculated using TCRdist. y-axis represents the likelihood for pairs of cells with a given TCR
410 distance to be of the same T helper subset, normalized to the prior probability of any two cells
411 belonging to that subset (see **Methods**). ‘*****’ refers to an adjusted p-value of <0.0001 by a two-
412 sided Chi-square proportion test with one degree of freedom, ‘****’ refers to p-value of <0.001, and
413 ‘**’ refers to p-value of <0.01. Data represent combined data from all patients at all timepoints (**a**-
414 **d**).



416

417 **Figure 4. Th1 and Th2, but not Tfh, subsets are suppressed by OIT. a,** Mean Th1, Th2 and
 418 Th17 module expression over time for treatment-group patients. Each data point represents the
 419 mean of all CD154+ cells for a given patient at a given time point. ‘*’ refers to an adjusted p-value

420 of <0.05 by a Wilcoxon signed-rank test. **b**, Fractional expression of Th2, Th1, and Th17 modules
421 within clonotypes of T helper subtypes over time. Fractional clonal expression is defined as the
422 proportion of cells within each clonotype at a given time point expressing their respective module.
423 Each data point represents the cells of an individual expanded clonotype from one patient at one
424 timepoint. **c**, Degree of suppression in Th2A-like clones by clinical group. Ratio of mean Th2
425 module expression in Th2A-like clones from each patient was calculated between buildup (BU)
426 and maintenance (MN). Spearman's rho and p-value (** refers to p-value < 0.05) are from a
427 Spearman correlation test between ratio and outcome within the treatment group (assigning TO
428 as 2, PT as 1, and TF as 0). **d**, Principal component 1 (PC1) score of CD154+ cells by outcome.
429 A principal components analysis was done using the 50 gene modules as features and all CD154+
430 cells at baseline as the input data. Each data point represents the mean PC1 score of all CD154+
431 cells from a single patient at a single timepoint. Black-outlined points represent the baseline
432 timepoint. ** refers to an adjusted p-value of <0.05 by a Wilcoxon rank-sum test, *** refers to
433 adjusted p-value of <0.005 , and **** refers to adjusted p-value of <0.0005 . **e**, Top 5 gene module
434 loadings in PC1. Bar heights represent the magnitude of each contribution to PC1. Further details
435 of each gene module are available in Supplementary Figures 3 and 4.
436

437 **References**

- 438 1. Gupta, R. S. *et al.* The prevalence, severity, and distribution of childhood food allergy in
439 the United States. *Pediatrics* **128**, (2011).
- 440 2. Sicherer, S. H. & Sampson, H. A. Food allergy: A review and update on epidemiology,
441 pathogenesis, diagnosis, prevention, and management. *J. Allergy Clin. Immunol.* **141**,
442 41–58 (2018).
- 443 3. Vickery, B. P. *et al.* AR101 Oral Immunotherapy for Peanut Allergy. *N. Engl. J. Med.* **379**,
444 1991–2001 (2018).
- 445 4. Patil, S. U. *et al.* Peanut oral immunotherapy transiently expands circulating Ara h 2–
446 specific B cells with a homologous repertoire in unrelated subjects. *J. Allergy Clin.*
447 *Immunol.* **136**, 125-134.e12 (2015).
- 448 5. Vickery, B. P., Chin, S. & Burks, A. W. Pathophysiology of Food Allergy. *Pediatr. Clin.*
449 *North Am.* **58**, 363–376 (2011).
- 450 6. Prussin, C., Yin, Y. & Upadhyaya, B. TH2 heterogeneity: Does function follow form? *J.*
451 *Allergy Clin. Immunol.* **126**, 1094–1098 (2010).
- 452 7. Sampath, V. & Nadeau, K. C. Newly identified T cell subsets in mechanistic studies of
453 food immunotherapy. *Journal of Clinical Investigation* **129**, 1431–1440 (2019).
- 454 8. Wambre, E. *et al.* A phenotypically and functionally distinct human TH2 cell
455 subpopulation is associated with allergic disorders. *Sci. Transl. Med.* **9**, eaam9171
456 (2017).
- 457 9. Gowthaman, U. *et al.* Identification of a T follicular helper cell subset that drives
458 anaphylactic IgE. *Science (80-.)*. **365**, eaaw6433 (2019).
- 459 10. Mitson-Salazar, A. *et al.* Hematopoietic prostaglandin D synthase defines a
460 proeosinophilic pathogenic effector human T H 2 cell subpopulation with enhanced
461 function. *J. Allergy Clin. Immunol.* **137**, 907-918.e9 (2016).
- 462 11. Rüter, B. *et al.* Expansion of the CD4+ effector T-cell repertoire characterizes peanut-

- 463 allergic patients with heightened clinical sensitivity. *J. Allergy Clin. Immunol.* **145**, 270–
464 282 (2020).
- 465 12. Haribhai, D. *et al.* A requisite role for Induced Regulatory T cells in Tolerance Based on
466 Expanding Antigen Receptor Diversity. *Immunity* **35**, 109–122 (2011).
- 467 13. Chinthrajah, R. S. *et al.* Sustained outcomes in oral immunotherapy for peanut allergy
468 (POISED study): a large, randomised, double-blind, placebo-controlled, phase 2 study.
469 *Lancet* **394**, 1437–1449 (2019).
- 470 14. Blumchen, K. *et al.* Oral peanut immunotherapy in children with peanut anaphylaxis. *J.*
471 *Allergy Clin. Immunol.* **126**, 83-91.e1 (2010).
- 472 15. Vickery, B. P. *et al.* Sustained unresponsiveness to peanut in subjects who have
473 completed peanut oral immunotherapy. *J. Allergy Clin. Immunol.* **133**, 468-475.e6 (2014).
- 474 16. Blumchen, K. *et al.* Efficacy, Safety, and Quality of Life in a Multicenter, Randomized,
475 Placebo-Controlled Trial of Low-Dose Peanut Oral Immunotherapy in Children with
476 Peanut Allergy. *J. Allergy Clin. Immunol. Pract.* **7**, 479-491.e10 (2019).
- 477 17. Kim, E. H. *et al.* Sublingual immunotherapy for peanut allergy: clinical and immunologic
478 evidence of desensitization. *J. Allergy Clin. Immunol.* **127**, 640–6.e1 (2011).
- 479 18. Ryan, J. F. *et al.* Successful immunotherapy induces previously unidentified allergen-
480 specific CD4+ T-cell subsets. *Proc. Natl. Acad. Sci. U. S. A.* **113**, E1286–E1295 (2016).
- 481 19. Frischmeyer-Guerrerio, P. A. *et al.* Mechanistic correlates of clinical responses to
482 omalizumab in the setting of oral immunotherapy for milk allergy. *J. Allergy Clin. Immunol.*
483 **140**, 1043-1053.e8 (2017).
- 484 20. Syed, A. *et al.* Peanut oral immunotherapy results in increased antigen-induced
485 regulatory T-cell function and hypomethylation of forkhead box protein 3 (FOXP3). *J.*
486 *Allergy Clin. Immunol.* **133**, 500-510.e11 (2014).
- 487 21. Varshney, P. *et al.* A randomized controlled study of peanut oral immunotherapy: Clinical
488 desensitization and modulation of the allergic response. *J. Allergy Clin. Immunol.* **127**,

- 489 654–660 (2011).
- 490 22. Weissler, K. A. *et al.* Identification and analysis of peanut-specific effector T and
491 regulatory T cells in children allergic and tolerant to peanut. *J. Allergy Clin. Immunol.* **141**,
492 1699-1710.e7 (2018).
- 493 23. Wang, W. *et al.* Transcriptional changes in peanut-specific CD4+ T cells over the course
494 of oral immunotherapy. *Clin. Immunol.* **219**, 108568 (2020).
- 495 24. Wambre, E. Effect of allergen-specific immunotherapy on CD4+ T cells. *Current Opinion*
496 *in Allergy and Clinical Immunology* **15**, 581–587 (2015).
- 497 25. Tordesillas, L. & Berin, M. C. Mechanisms of Oral Tolerance. *Clinical Reviews in Allergy*
498 *and Immunology* **55**, 107–117 (2018).
- 499 26. Chiang, D. *et al.* Single-cell profiling of peanut-responsive T cells in patients with peanut
500 allergy reveals heterogeneous effector T H 2 subsets. *J. Allergy Clin. Immunol.* **141**,
501 2107–2120 (2018).
- 502 27. Bacher, P. *et al.* Regulatory T Cell Specificity Directs Tolerance versus Allergy against
503 Aeroantigens in Humans. *Cell* **167**, 1067-1078.e16 (2016).
- 504 28. Aguet, F. *et al.* Genetic effects on gene expression across human tissues. *Nature* **550**,
505 204–213 (2017).
- 506 29. Kunnath-Velayudhan, S. *et al.* Transcriptome Analysis of Mycobacteria-Specific CD4 + T
507 Cells Identified by Activation-Induced Expression of CD154. *J. Immunol.* **199**, 2596–2606
508 (2017).
- 509 30. Commandeur, S. *et al.* Clonal Analysis of the T-Cell Response to In Vivo Expressed
510 Mycobacterium tuberculosis Protein Rv2034, Using a CD154 Expression Based T-Cell
511 Cloning Method. *PLoS One* **9**, e99203 (2014).
- 512 31. Gierahn, T. M. *et al.* Seq-Well: portable, low-cost RNA sequencing of single cells at high
513 throughput. *Nat. Methods* **14**, 395–398 (2017).
- 514 32. Tu, A. A. *et al.* TCR sequencing paired with massively parallel 3' RNA-seq reveals

- 515 clonotypic T cell signatures. *Nat. Immunol.* **20**, 1692–1699 (2019).
- 516 33. Witten, D. M., Tibshirani, R. & Hastie, T. A penalized matrix decomposition, with
517 applications to sparse principal components and canonical correlation analysis.
518 *Biostatistics* **10**, 515–534 (2009).
- 519 34. Kim, C. J. *et al.* The Transcription Factor Ets1 Suppresses T Follicular Helper Type 2 Cell
520 Differentiation to Halt the Onset of Systemic Lupus Erythematosus. *Immunity* **49**, 1034-
521 1048.e8 (2018).
- 522 35. NovalRivas, M. *et al.* Regulatory T cell reprogramming toward a Th2-Cell-like lineage
523 impairs oral tolerance and promotes food allergy. *Immunity* **42**, 512–523 (2015).
- 524 36. Velu, V. *et al.* Induction of Th1-Biased T Follicular Helper (Tfh) Cells in Lymphoid Tissues
525 during Chronic Simian Immunodeficiency Virus Infection Defines Functionally Distinct
526 Germinal Center Tfh Cells. *J. Immunol.* **197**, 1832–1842 (2016).
- 527 37. James, K. R. *et al.* Distinct microbial and immune niches of the human colon. *Nat.*
528 *Immunol.* **21**, 343–353 (2020).
- 529 38. Dash, P. *et al.* Quantifiable predictive features define epitope-specific T cell receptor
530 repertoires. *Nature* **547**, 89–93 (2017).
- 531 39. Hayes, S. M., Li, L. Q. & Love, P. E. TCR signal strength influences $\alpha\beta/\gamma\delta$ lineage fate.
532 *Immunity* **22**, 583–593 (2005).
- 533 40. Daniels, M. A. & Teixeira, E. TCR Signaling in T Cell Memory. *Front. Immunol.* **6**, 617
534 (2015).
- 535 41. Snook, J. P., Kim, C. & Williams, M. A. TCR signal strength controls the differentiation of
536 CD4+ effector and memory T cells. *Sci. Immunol.* **3**, (2018).
- 537 42. Tubo, N. J. *et al.* Single naive CD4+ T cells from a diverse repertoire produce different
538 effector cell types during infection. *Cell* **153**, 785–796 (2013).
- 539 43. Kotov, D. I. *et al.* TCR Affinity Biases Th Cell Differentiation by Regulating CD25, Eef1e1,
540 and Gbp2. *J. Immunol.* **202**, 2535–2545 (2019).

- 541 44. Stockinger, B. & Omenetti, S. The dichotomous nature of T helper 17 cells. *Nature*
542 *Reviews Immunology* **17**, 535–544 (2017).
- 543 45. Choy, D. F. *et al.* TH2 and TH17 inflammatory pathways are reciprocally regulated in
544 asthma. *Sci. Transl. Med.* **7**, 301ra129 (2015).
- 545 46. Hirahara, K. & Nakayama, T. CD4+ T-cell subsets in inflammatory diseases: Beyond the
546 Th1/Th2 paradigm. *International Immunology* **28**, 163–171 (2016).
- 547 47. Luce, S., Chinthrajah, S., Lyu, S.-C., Nadeau, K. C. & Mascarell, L. Th2A and Th17 cell
548 frequencies and regulatory markers as follow-up biomarker candidates for successful
549 multifood oral immunotherapy. *Allergy* **75**, 1513–1516 (2020).
- 550 48. Guttman-Yassky, E. *et al.* GBR 830, an anti-OX40, improves skin gene signatures and
551 clinical scores in patients with atopic dermatitis. *J. Allergy Clin. Immunol.* **144**, 482-493.e7
552 (2019).
- 553 49. Seshasayee, D. *et al.* In vivo blockade of OX40 ligand inhibits thymic stromal
554 lymphopietin driven atopic inflammation. *J. Clin. Invest.* **117**, 3868–3878 (2007).
- 555 50. Adamczyk, A. *et al.* Differential expression of GPR15 on T cells during ulcerative colitis.
556 *JCI insight* **2**, (2017).
- 557 51. Ovadia, A., Sharfe, N., Hawkins, C., Laughlin, S. & Roifman, C. M. Two different STAT1
558 gain-of-function mutations lead to diverse IFN- γ -mediated gene expression. *npj Genomic*
559 *Med.* **3**, 23 (2018).
- 560 52. Guidance for Industry: Pyrogen and Endotoxins Testing: Questions and Answers | FDA.
561 Available at: [https://www.fda.gov/regulatory-information/search-fda-guidance-](https://www.fda.gov/regulatory-information/search-fda-guidance-documents/guidance-industry-pyrogen-and-endotoxins-testing-questions-and-answers)
562 [documents/guidance-industry-pyrogen-and-endotoxins-testing-questions-and-answers.](https://www.fda.gov/regulatory-information/search-fda-guidance-documents/guidance-industry-pyrogen-and-endotoxins-testing-questions-and-answers)
563 (Accessed: 2nd March 2021)
- 564 53. Macosko, E. Z. *et al.* Highly Parallel Genome-wide Expression Profiling of Individual Cells
565 Using Nanoliter Droplets. *Cell* **161**, 1202–1214 (2015).
- 566 54. McInnes, L., Healy, J. & Melville, J. UMAP: Uniform Manifold Approximation and

567 Projection for Dimension Reduction. (2018).

568

569

570 **Methods**

571 **Patients.** Peanut-allergic individuals age 7 years and older were enrolled in a peanut OIT trial
572 (NCT01750879) at the Food Allergy Center at Massachusetts General Hospital. All subjects
573 were recruited with informed consent, and the study was approved by the Institutional Review
574 Board of Partners Healthcare (protocol 2012P002153). Study participants with a previous
575 diagnosis of peanut allergy, a history of peanut-induced reactions consistent with immediate
576 hypersensitivity, and confirmatory peanut- and Ara h 2–specific serum IgE concentrations
577 (peanut-specific IgE > 5 kU/L, Ara h 2–specific IgE > 0.35 kU/L; ImmunoCAP; Thermo Fisher,
578 Waltham, MA) underwent a double-blind placebo-controlled food challenge (DBPCFC).
579 Increasing peanut protein doses were administered every 20 minutes to a maximum dose of
580 300 mg according to the following schedule: 3, 10, 30, 100, and 300 mg, for a cumulative total
581 of 443 mg. Patients who had an objective allergic reaction during the challenge were eligible for
582 inclusion in the study.

583 **Oral immunotherapy (OIT) study.** The main objective of this phase I/II, double-blind placebo-
584 controlled, interventional study was to provide safety and mechanistic data on OIT for people with
585 IgE-mediated peanut allergy. Enrolled patients were randomized to receive either treatment
586 (peanut flour) or placebo (roasted oat flour) at a ratio of 3:1. Treatment consisted of a modified-
587 rush protocol, followed by a build-up phase lasting for 44 weeks or when the patient reached
588 4000mg, whichever came first. Treatment dose was administered daily, and dosing escalation
589 was incremental, based on previous OIT studies⁸, occurring every two weeks. After the buildup
590 phase, patients entered a maintenance phase in which treatment was continued at the top
591 tolerated dose for each patient for 12 weeks. Finally, patients underwent an avoidance phase, 12
592 weeks off therapy while strictly avoiding dietary peanut protein, in order to assess the durability
593 of any desensitization resulting from OIT. During each phase of the study, a blood sample was
594 taken, for four samples total per patient: 2 weeks prior to the start of treatment at baseline, 14

595 weeks into the buildup phase, 8 weeks into the maintenance phase, and 8 weeks into the
596 avoidance phase.

597 Clinical assessments were made by double-blind placebo-controlled food challenge at baseline
598 (DBPCFC1), at the end of 12 weeks of maintenance therapy (DBPCFC2), and at the end of 12
599 weeks of avoidance²¹ (DBPCFC3). Clinical outcomes were defined as: treatment failure (failure
600 to achieve the minimum maintenance dose (600 mg) of peanut protein by 12 months, or an
601 eliciting dose less than 1443 mg at DBPCFC2, or less than 443mg at DBPCFC3, OR less than
602 10-fold more than at DBPCFC1); partial tolerance (eliciting dose less than 4430mg at DBPCFC3
603 but at least 443 mg AND more than 10-fold more than at DBPCFC1); and tolerance (ingestion of
604 4430 mg of peanut protein at DBPCFC3 without symptoms).

605 **Cell purification and sorting.** After a blood sample was collected, PBMCs were isolated by
606 density gradient centrifugation (Ficoll-Paque Plus; GE Healthcare) and cryopreserved in FBS with
607 10% DMSO. After the study was completed, for each of the 12 patients, PBMCs from all four time
608 points (15-30 x 10⁶ PBMCs per timepoint) were simultaneously thawed, washed with PBS, and
609 cultured in AIM-V medium (Gibco) with 100 µg/ml peanut protein extract for 20h, at a density of 5
610 x 10⁶ PBMCs in 1 mL medium per well in 24-well plates. Peanut protein extract was prepared by
611 agitation of defatted peanut flour (Golden Peanut and Tree Nuts, Alpharetta, GA) with PBS,
612 centrifugation, and sterile-filtering. Endotoxin concentration in the peanut protein extract was
613 assessed to be 6 EU/mg, using a LAL Endotoxin Quantitation kit (Thermo Fisher; cat. no. 88282).
614 This is lower than the concentration in commercially available endotoxin-depleted preparations of
615 the purified peanut proteins Ara h 1 and Ara h 2 (Indoor Biotechnologies; LTN-AH1-1 and LTN-
616 AH2-1). Furthermore, the endotoxin concentration in the PBMC cultures with peanut protein
617 extract was 0.6 EU/ml, which is comparable to the endotoxin limit for eluates from medical devices
618 (0.5 EU/ml) as determined by the FDA⁵². Anti-CD154-PE antibody (BD Biosciences; clone
619 TRAP1) was added to the cultures at a 1:50 dilution (20 µl/well) for the last 3h. After harvesting,
620 the cells were labeled with anti-CD3-AF700 (BD Biosciences; UCHT1), anti-CD4-APC-Cy7 (BD

621 Biosciences; RPA-T4), anti-CD45RA-PE-Cy7 (BD Biosciences; HI100), anti-CD154-PE (BD
622 Biosciences; TRAP1), anti-CD137-APC (BD Biosciences; clone 4B4-1), and Live/Dead Fixable
623 Blue stain (Thermo Fisher; cat. no. L23105). Cells were then sorted with a FACSAria Fusion
624 instrument (BD Biosciences). Cells were gated as live singlet CD3+CD4+CD45RA- and then
625 sorted as either CD154+CD137+/- (referred to as “CD154+”), CD154-CD137+ (“CD137+”), or
626 CD154-CD137-.

627 **Single-cell RNA-Seq.** Sorted subsets of CD4 memory T cells were processed for single-cell RNA
628 sequencing using the Seq-Well platform as previously described³¹. A portion of each cDNA library
629 was reserved for paired TCR α/β enrichment. The rest was barcoded and amplified using the
630 Nextera XT kit and sequenced on the Illumina NovaSeq.

631 Raw read processing was performed as in Macosko et al⁵³. Briefly, sequencing reads were
632 aligned to the ‘hg38’ reference human genome, collapsed by unique molecular identifier (UMI),
633 and counted to obtain a digital gene expression matrix of cells versus genes. These counts were
634 then filtered to exclude any cells with fewer than 1000 genes or 2000 UMIs and normalized by
635 library size per cell and a log₂ transformation. For the rare T helper subsets analysis which
636 required more cells, a filter of 500 genes and 1000 UMIs was used.

637 **Paired single-cell TCR α/β sequencing.** Paired TCR sequencing was performed according to Tu
638 et al³². Briefly, following cDNA amplification, biotinylated capture probes for human TRAC and
639 TRBC regions were annealed to cDNA. Magnetic streptavidin beads were used to enrich the
640 bound TCR sequences, which were then further amplified using human V-region primers and
641 prepared for sequencing using Nextera sequencing handles. Libraries were sequenced on an
642 Illumina MiSeq using 150bp-length reads.

643 TCR sequencing reads were preprocessed according to Tu et al³². In short, reads were mapped
644 to TCRV and TCRJ IMGT reference sequences via IgBlast, and V and J calls with “strong plurality”
645 (wherein the ratios of the most frequent V and J calls to the second most frequent calls were at

646 least 0.6) were retained. CDR3 sequences were called by identifying the 104-cysteine and 118-
647 phenylalanine according to IMGT references and translating the amino acid sequences in
648 between those residues. Processed TCR sequences were then paired with the single-cell
649 transcriptome data via the cell barcodes.

650 **Visualization of single-cell RNA-Seq data.** Visualization of single-cell transcriptomes was done
651 with UMAP⁵⁴ (uniform manifold approximation and projection) with the Python package “scanpy”.
652 Prior to visualization, the normalized gene expression data was transformed using a standard
653 “regress-out” approach to mitigate batch effects: a multiple linear regression was performed on
654 all genes with two covariates that could be batch-associated (numbers of transcripts per cell, and
655 percent of transcripts aligning to the mitochondrial chromosome). The residuals from this
656 regression were taken as the transformed data. Next, a principal components analysis was
657 performed, and the top 10 components were used to generate a UMAP visualization.

658 **Gene module discovery.** Coexpressed gene modules were generated based on a sparse PCA
659 approach described by Witten et al and implemented in the R package “PMA”³³. This
660 unsupervised method employs an L1 norm penalty on loadings in each component to introduce
661 sparsity. Prior to running sparse PCA, the gene expression matrix was randomly downsampled
662 to have an equal number of cells from all samples, to prevent the results from being skewed by a
663 subset of the samples. Genes were filtered down to the union of immune genes (defined by the
664 set of gene lists available on ImmPort at <https://www.immport.org/shared/genelists>) and the
665 variable genes in the dataset (defined using the R package “Seurat”). Finally, the gene expression
666 data was scaled with respect to genes, and sparse PCA was run using the command “SPC”.
667 Gene module scores were calculated as the scaled gene expression input matrix multiplied by
668 the outputted loadings matrix “v”. The first 50 gene modules were retained for downstream
669 analysis.

670 Cells were classified as “expressing” or “not expressing” a module using a simple thresholding
671 strategy. The distribution of module scores of CD154-CD137- cells was used as a negative

672 control, and a threshold was set at the point where 0.2% of CD154-CD137- cells were in the
673 positive population. Cells with a module score above the threshold were labeled as “expressing”
674 that module. Modules in which at least 60% of the expressing cells were from a single patient
675 were removed from downstream analysis.

676 **Identification of T helper subtypes.** All CD154+ and CD137+ cell transcriptomes were classified
677 as Th1, Th2, or Th17 using the criteria for module expression detailed above (see **Gene module**
678 **discovery**) for the Th1, Th2, and Th17 gene modules. If a cell expressed more than one Th
679 module, it was assigned to the module with the highest z-score (compared to the distribution of
680 all CD154+ and CD137+ cells). Then, each individual Th class (Th1, Th2, and Th17 cells) was
681 separately visualized by UMAP and clustered by Louvain clustering using the R package ‘Seurat’.

682 **Distance analysis of TCR sequences.** Pairwise distance of TCR β CDR3 sequences was
683 evaluated using the TCRdist method published by Dash et al³⁸. Briefly, for two TCR β CDR3 amino
684 acid sequences of the same length, each residue position was compared, and a penalty was
685 assessed for every mismatch. The penalty for two different amino acid residues i and j was
686 assessed using the BLOSUM62 matrix and was defined as $\min(4 - \text{BLOSUM62}[i, j], 4)$. Each
687 substitution thus incurred a penalty between 1 and 4. The overall distance between two CDR3s
688 was calculated as the sum of penalties at all positions. In the case of two CDR3s of unequal
689 length, the sequences were aligned in all possible ways and the minimum overall penalty was
690 taken, with each gap incurring a penalty of 8.

691 **Likelihood-based association between TCR and T helper subtype.** Likelihood-based analysis
692 was used to determine the tightness of association between T helper subset and TCR β CDR3
693 sequence. A log-likelihood ratio was defined as $\log_2(P/P_0)$, where P was the probability of two
694 cells being of the same T helper subset if they were drawn randomly from all cells sharing the
695 same TCR β CDR3 sequence (without replacement), and P_0 was the probability of two cells being
696 of the same T helper subset if they were drawn randomly from all cells. P_0 represents the prior

697 probability without the constraint of TCR information; thus, the ratio P/P_0 represents the gain in
698 likelihood due to the knowledge of TCR sequence. This analysis was constrained to consider all
699 pairs of cells within the same patient.

700 **Longitudinal analysis of clonotypes.** Temporal analysis of individual clonotypes over the
701 course of OIT involved two analyses: 1) obtaining the distribution of timepoints at which each
702 clonotype was detected, and 2) assessing module expression of clonotypes within T helper
703 subtypes. For the former, CD154+ or CD137+ clones were filtered to those with at least 4 cells in
704 that sorted subset. Then, the timepoints covered by the cells was tabulated and the clonotype
705 was classified as having a specific temporal pattern (e.g. “BL, BU, AV”). For the latter, clonotypes
706 were filtered down to those with at least 2 cells in the combined CD154+ and CD137+
707 compartments. Each clonotype was then assigned to a T helper subtype (or no subtype) based
708 on the most frequent T subtype that its cells mapped to (see **Identification of T helper**
709 **subtypes**). At each timepoint, the fraction of cells within each clonotype expressing the relevant
710 module (Th1, Th2, or Th17) was counted, relative to the total number of cells of that clonotype at
711 that timepoint. Fractional expression was used instead of module scores in order to normalize for
712 clonotype- or patient-driven differences in dynamic range of module expression.

713 **Baseline signature of all modules using PCA.** Principal component analysis was used to
714 identify broad immune signatures associated with clinical outcome. Mean module scores of the
715 50 gene modules (minus the 7 modules associated with a single patient; see **Gene module**
716 **discovery**) were computed for each patient at each timepoint. Averages at baseline were used
717 to compute the principal components. The first principal component (“PC1”), or the component
718 explaining the largest amount of variance, was then applied to module averages of other
719 timepoints.

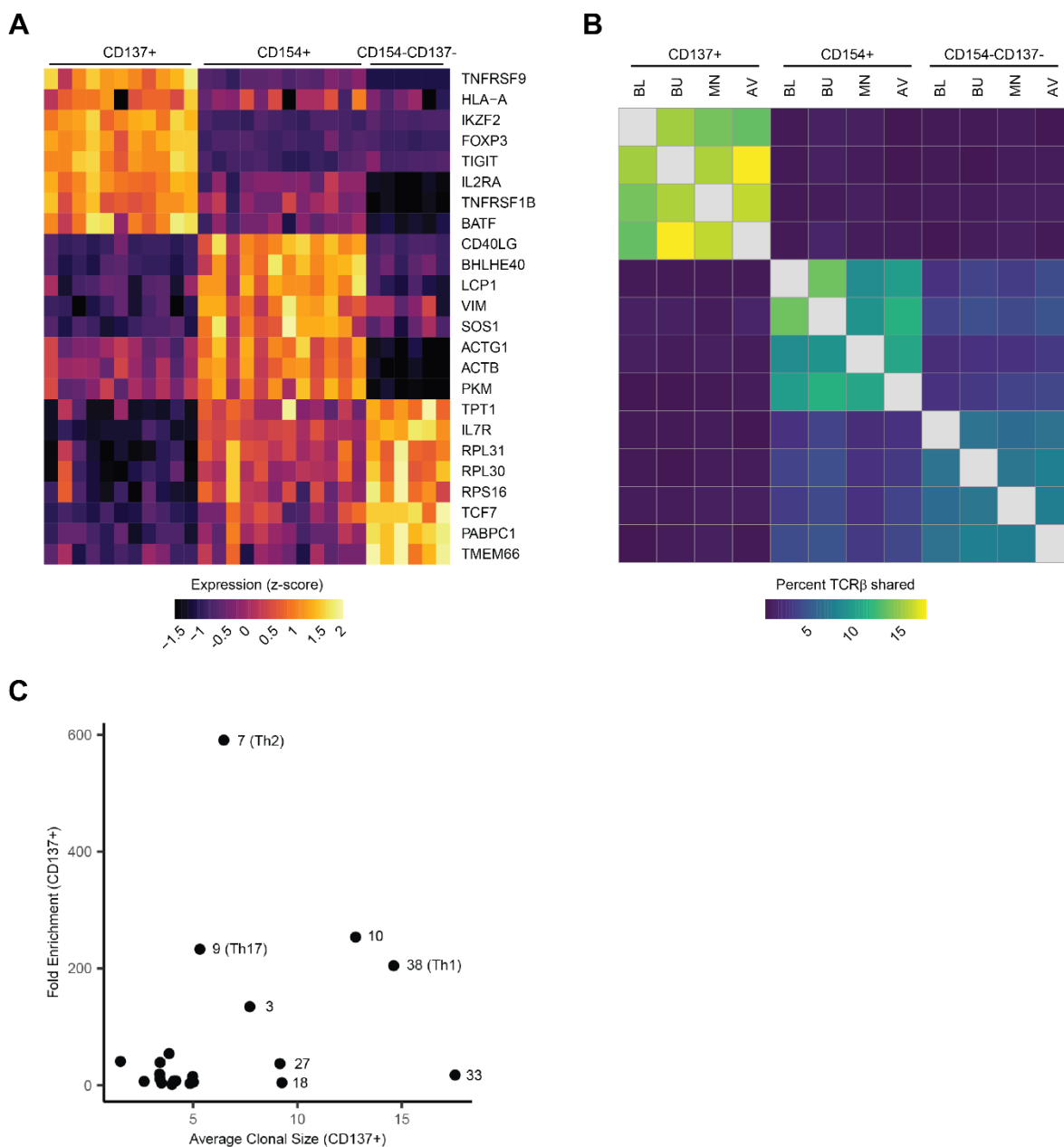
720 **Spearman correlation of treatment outcome and module expression.** To investigate whether
721 treatment outcome was correlated with expression of modules enriched in PC1, we assigned
722 numerical values to each of the outcomes (TO as 2, PT as 1, and TF as 0) to represent an ordinal

723 relationship between the outcomes. Spearman correlation between mean module expression (by
724 patient and cell subset) and outcomes was calculated. Corresponding unadjusted p-values were
725 reported.

726 **Statistical analyses.** All statistical tests were performed as two-sided tests unless otherwise
727 noted. Box plots were plotted with the standard visualization of 25th and 75th percentile for the
728 lower and upper hinges, and at most 1.5 times the interquartile range for the whisker lengths.

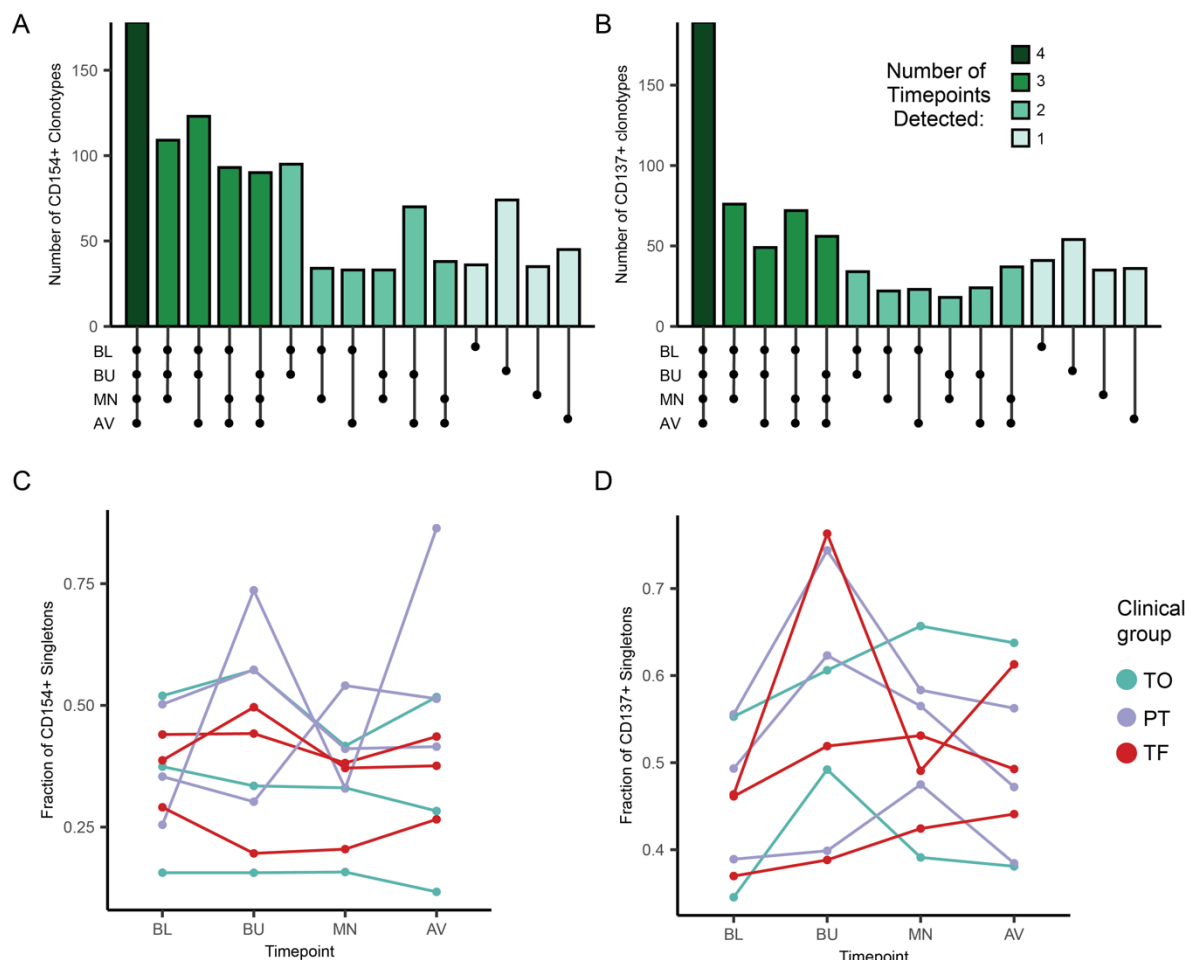
729 **Data availability.** FASTQ file format data related to human samples will be available through
730 dbGaP under accession number phs001897.v1.p1. Processed gene expression and associated
731 TCR clonotype data will be available through GEO under accession number GSE158667.
732 Processed data files and associated meta data tables for Figures 1-4 will be made available on
733 <https://github.com/mitlovelab/>, or upon request.

734 **Code availability.** R, python, and Matlab scripts for processing TCR sequencing data and
735 generating all analyses, as well as all updates, will be made available on
736 https://github.com/mitlovelab or upon request.



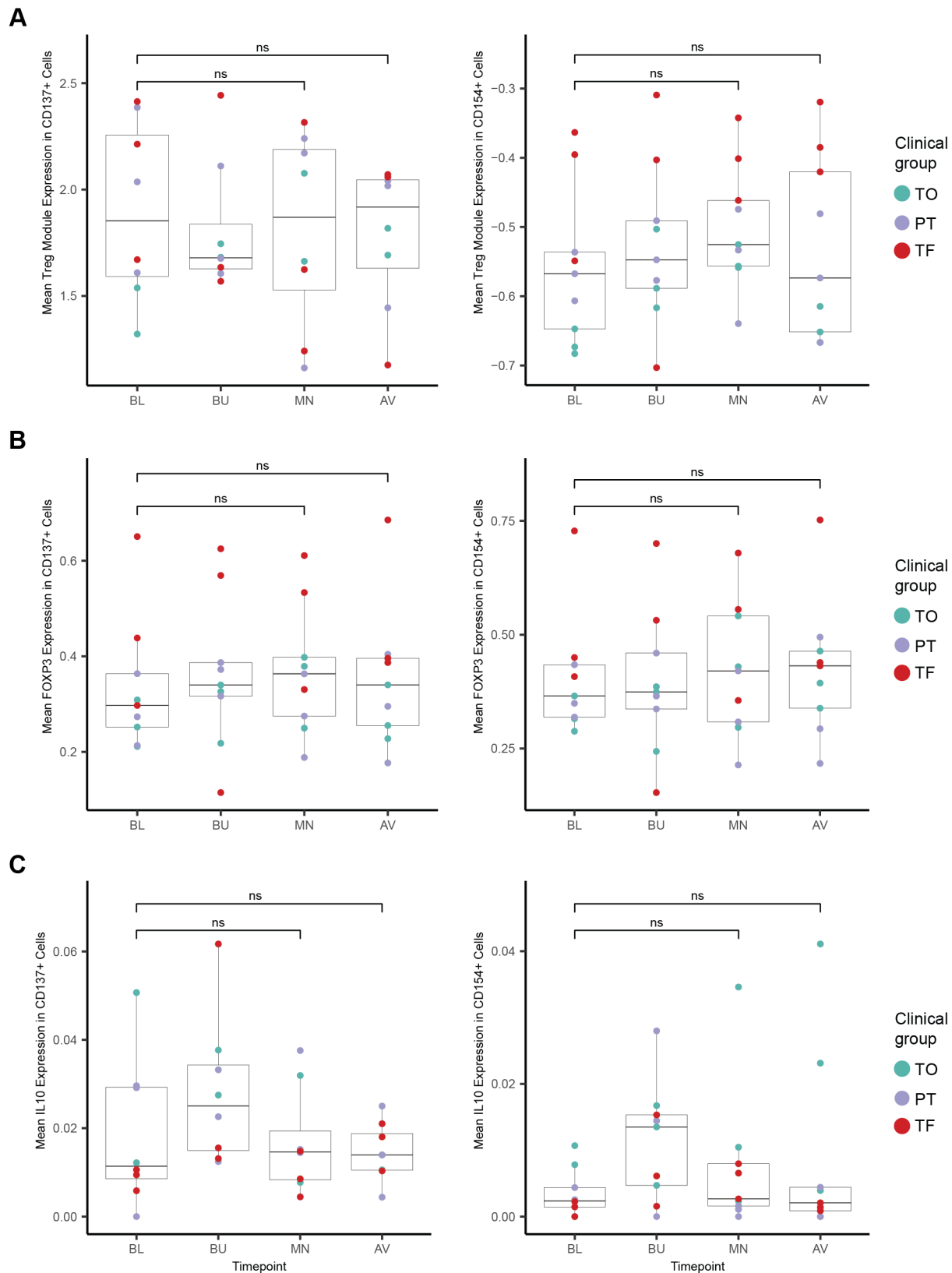
738 **Extended Data 1. a**, Top differentially expressed genes between the sorted subsets. Each
 739 column represents the scaled average gene expression of cells from a single patient. Genes were
 740 selected using ROC test. **b**, Percent of TCRβ sequences shared between time points and all
 741 sorted subsets. ‘Percent shared’ is defined as the number of unique TCRβ sequences detected
 742 in both conditions, divided by the geometric mean of the number of unique TCRβ sequences in
 743 each of the two conditions. Sequences from all treatment-group patients were pooled. Patients
 744 without recovered TCR sequences from all three sorted subsets were excluded from the analysis.

745 **c**, Mean clonal size and fold-change in mean module scores (compared to module-expressing
746 CD154-CD137- cells) in CD137+ cells expressing each gene module. Cells were classified as
747 'expressing' each module or not, relative to background expression (**Methods**). Clonal size was
748 calculated with respect to all cells in the dataset.



750

751 **Extended Data 2. a-b**, Number of TCR β clonotypes detected at every possible combination of
 752 timepoints in (a) CD154+ and (b) CD137+ cells. Clones from all treatment-group patients with at
 753 least 4 cells were included. **c-d**, Fraction of singletons (clonotypes with clonal size of one)
 754 detected within each patient and at each timepoint in (c) CD154+ and (d) CD137+ cells.



756

757 **Extended Data 3. a**, Average expression of Treg module (module 1) by patient and timepoint

758 within CD137+ (left) and CD154+ (right) cells. **b**, Average expression of *FOXP3* by patient and

759 timepoint within CD137+ (left) and CD154+ (right) cells. **c**, Average expression of *IL10* by patient
760 and timepoint within CD137+ (left) and CD154+ (right) cells. Adjusted p-values calculated by
761 Wilcoxon rank-sum test (**a-c**).
762